

# Gravitational Reheating

Md Riajul Haque\* and Debaprasad Maity, †

*Department of Physics, Indian Institute of Technology, Guwahati, India*

In this letter, we show for the first time that the perfect state of our present universe can be obtained through gravitational interaction between inflaton and all fundamental fields during reheating without invoking new physics. Our analysis revealed that gravitational reheating is consistent for a very restricted class of inflation models and narrow ranges of reheating temperature and dark matter mass.

PACS numbers:

**Introduction** Reheating is a natural physical phenomenon after inflation. Dark matter (DM) and all standard model (SM) fields must be produced during this phase. In the simplest scenario, when a single scalar field drives inflation, shift symmetry is expected to play an important role in the nature of coupling among inflaton and any the other fields, and this symmetry must naturally suppress it. However, all fields are naturally coupled gravitationally, and when the energy scale of any physical processes such as reheating is as large as  $\sim 10^{15}$  GeV, gravity mediated decay process may be strong and sufficient to reheat the universe. This is the possibility we will explore in this letter. We will name it gravitational reheating (GRe). In this phase, DM mass is the only free parameter except, of course, the inflationary parameters. We will see how such less freedom naturally makes GRe a unique mechanism as compared to reheating scenarios discussed so far in the literature [1, 2]. All the massless decay products from inflaton will be collectively called radiation, and massive ones are DM. Given the present state of the universe, GRe turned out to be consistent with a very limited class of inflation models and a narrow range of DM masses. GRe is insensitive to any new physics in the radiation and DM sector. However, if DM couples with the radiation bath, gravitational production sets the maximum limit on the DM mass [3]. It is the s-channel graviton exchange process through which inflaton converts its energy to radiation and DM during reheating. Graviton exchange processes between radiation bath and DM will be ignored due to its subdominant contribution (see detailed study in [3–5]). The dynamical equations for GRe are [6]

$$\begin{aligned}\dot{\rho}_\phi + 3H(1 + \omega_\phi)\rho_\phi + \Gamma_\phi^T \rho_\phi(1 + \omega_\phi) &= 0, \\ \dot{\rho}_R + 4H\rho_R - \Gamma_{\phi\phi \rightarrow RR}^{Rad} \rho_\phi(1 + \omega_\phi) &= 0, \\ \dot{n}_Y + 3Hn_Y - \frac{\Gamma_{\phi\phi \rightarrow YY}^{DM}}{m_\phi} \rho_\phi(1 + \omega_\phi) &= 0\end{aligned}$$

where,  $(\rho_\phi, \rho_R, n_Y)$  are inflaton energy density, radiation energy density and dark matter number density

respectively. The total inflation decay width is  $\Gamma_\phi^T = \Gamma_{\phi\phi \rightarrow RR}^{Rad} + \Gamma_{\phi\phi \rightarrow YY}^{DM}$ . The gravitational decay width of inflaton to fundamental fields are [7–11],

$$\begin{aligned}\Gamma_{\phi\phi \rightarrow SS} &= \frac{\rho_\phi m_\phi}{1024 \pi M_p^4} \left(1 + \frac{m_S^2}{2m_\phi^2}\right) \sqrt{1 - \frac{m_S^2}{m_\phi^2}}, \\ \Gamma_{\phi\phi \rightarrow ff} &= \frac{\rho_\phi m_f^2}{4096 \pi M_p^4 m_\phi} \left(1 - \frac{m_f^2}{m_\phi^2}\right)^{\frac{3}{2}}, \\ \Gamma_{\phi\phi \rightarrow XX} &= \frac{\rho_\phi m_\phi}{32768 \pi M_p^4} \left(4 + 4 \frac{m_X^2}{m_\phi^2} + 19 \frac{m_X^4}{m_\phi^4}\right) \sqrt{1 - \frac{m_X^2}{m_\phi^2}}.\end{aligned}\quad (0.1)$$

The symbols  $(R, Y)$  represent scalar  $(S)$ , fermion  $(f)$ , and vector particles  $(X)$ . Pauli spin blocking renders inflaton to fermion decay width proportional to the fermion mass  $m_f$ . This immediately indicates  $\Gamma_{\phi\phi \rightarrow ff}^{Rad} \ll \Gamma_{\phi\phi \rightarrow SS}^{Rad}, \Gamma_{\phi\phi \rightarrow XX}^{Rad}$ , as mass of the radiation constituents are small and hence, we ignore the fermionic contribution in radiation bath through out. Consequently,  $\Gamma_{\phi\phi \rightarrow RR}^{Rad} = \Gamma_{\phi\phi \rightarrow SS}^{Rad} + \Gamma_{\phi\phi \rightarrow XX}^{Rad} = (1 + \gamma)\Gamma_{\phi\phi \rightarrow SS}^{Rad}$ , with  $\gamma = 1/8$ . For DM, we analyze individual species. Massless graviton can also be part of the radiation bath through s-channel production, whose decay width will be suppressed due to its tensorial structure like the electromagnetic field. We ignore it in our analysis throughout. Finally, we also ignore gravitational  $\phi\phi \rightarrow \phi\phi$  channel production, which will be kinematically suppressed.

**Model of inflation:** To better understand the mechanism, along with the model-independent consideration, we also consider  $\alpha$ -attractor model with inflation potential [12, 13],

$$V(\phi) = \Lambda^4 \left[1 - e^{-\sqrt{\frac{2}{3\alpha}}\phi/M_p}\right]^{2n} \quad (0.2)$$

Where,  $(\alpha, n, \Lambda)$  are free parameters. Recent PLANCK [14] and BICEP/Keck [15] array combined results has put tight constraints on  $\alpha \sim (1, 12)$  [16]. Using BBN constraint on the primordial gravitational waves (PGWs), GRe will be shown to set even tighter constraint on  $\alpha$ . In this model, the inflationary observables assume remarkably simple form,  $1 - n_s \simeq 2/N_k, r \simeq 12\alpha/N_k^2$  [17]. Inflationary e-folding,  $N_k$  is defined for a CMB scale of interest  $k$  which crossed the Hubble radius near

\*riaju176121018@iitg.ac.in

†debu@iitg.ac.in

the beginning of inflation. After inflation ends, inflaton undergoes damped oscillation due to decay around the minimum where potential assumes power-law form,  $V(\phi) = \lambda \phi^{2n}$ , with  $\lambda = \Lambda^4 (2/(3\alpha M_p^2))^n$ . In order to describe reheating dynamics, we assume the equation of state (EoS) of the inflaton averaging over oscillation to be  $\omega_\phi \simeq (n-1)/(n+1)$ , and effective mass of inflaton  $m_\phi$  [18] in terms of energy density  $\rho_\phi$  as

$$m_\phi = \sqrt{\frac{2(1+\omega_\phi)(1+3\omega_\phi)}{(1-\omega_\phi)^2}} \lambda^{\frac{1-\omega_\phi}{2(1+\omega_\phi)}} \rho_\phi^{\frac{\omega_\phi}{1+\omega_\phi}} \quad (0.3)$$

**Computing reheating parameters:** In order to calculate quantities during reheating namely, reheating e-folding number ( $N_{re}$ ), reheating temperature ( $T_{re}$ ), and maximum radiation temperature ( $T_{max}$ ), we evaluate Eq.0.1 for radiation,

$$d(\rho_R A^4) = \Gamma_{\phi\phi \rightarrow RR}^{Rad} \rho_\phi (1+\omega_\phi) \frac{A^3 dA}{H} \quad (0.4)$$

where,  $A = a/a_{end}$  is normalized scale factor. Suffix "end" corresponds to the end of inflation. The production of radiation will depend on the inflaton energy density only, and hence, maximum production occurs at the beginning of reheating. During this early stage inflaton is naturally the dominating component. Neglecting decay term, therefore,  $\rho_\phi$  approximately evolves as  $\rho_\phi = \rho_\phi^{end} A^{-3(1+\omega_\phi)}$ , where,  $\rho_\phi^{end} = 3M_p^2 H_{end}^2$  denotes the inflaton energy density at the end of inflation. Consequently the Hubble parameter becomes,

$$H = \frac{\Lambda^2}{\sqrt{2}M_p} \left( \frac{2n}{2n+\sqrt{3\alpha}} \right)^n A^{-\frac{3}{2}(1+\omega_\phi)} = H_{end} A^{-\frac{3}{2}(1+\omega_\phi)}.$$

Using these the dynamical equation for the comoving radiation energy density transforms into,

$$d(\rho_R A^4) = 3M_p^2 H_{end} \Gamma_{\phi\phi \rightarrow RR}^{Rad} (1+\omega_\phi) A^{\frac{3}{2}(1+\omega_\phi)} dA.$$

With this we now calculate ( $N_{re}, T_{re}, T_{max}$ ). Considering the massless limit of the radiation constituents and using Eq.0.3 into, Eq.0.5, we find

$$\rho_R = \frac{9(1+\gamma) H_{end}^3 m_\phi^{end} (1+\omega_\phi)}{512\pi(1+15\omega_\phi) A^4} \left( 1 - A^{-\frac{1+15\omega_\phi}{2}} \right) \quad (0.5)$$

The above equation suggests that radiation production quickly happens at the beginning of reheating for large inflaton energy density and then freezes out. Competition between production and background expansion leads to a peak  $T_{max}$  in the radiation temperature, which is expressed as,

$$(T_{max})^4 = \frac{9(1+\gamma) H_{end}^3 m_\phi^{end} (1+\omega_\phi)}{512\beta\pi(1+15\omega_\phi) A_{max}^4} \left( 1 - A_{max}^{-\frac{1+15\omega_\phi}{2}} \right) \quad (0.6)$$

Here,  $\beta = \pi^2 g_*^{re}/30$  and  $g_*^{re}$  denotes the effective number of degrees of freedom associated with the radiation bath at the point of reheating. Where,  $A_{max} = ((9+15\omega_\phi)/8)^{\frac{2}{1+15\omega_\phi}}$ . End of reheating is defined at the point where,  $\rho_\phi = \rho_R$  as long as it satisfies BBN temperature bound. It turns out that when  $\omega_\phi < 1/3$ , the above condition is equivalent to  $H \simeq \Gamma_{\phi\phi \rightarrow RR}^{Rad}$ , which may not necessarily be true for  $\omega_\phi > 1/3$ . The reason behind this is that the inflaton dilutes itself much faster than its decay for higher EoS. Therefore, Eq.0.5 with the condition of reheating end one obtains the reheating e-folding number  $N_{re}$  as,

$$N_{re} = \frac{1}{3\omega_\phi - 1} \ln \left( \frac{512\pi M_p^2 (1+15\omega_\phi)}{3(1+\gamma) H_{end} m_\phi^{end} (1+\omega_\phi)} \right), \quad (0.7)$$

By using the above equation (Eq.0.7) one immediately computes the reheating temperature as,

$$T_{re} = \left( \frac{9(1+\gamma) H_{end}^3 m_\phi^{end} (1+\omega_\phi)}{512\beta\pi(1+15\omega_\phi)} e^{-4N_{re}} \right)^{1/4} \quad (0.8)$$

Furthermore, entropy conservation from the reheating end to present gives an additional important relation between ( $T_{re}, N_k$ ) as [1, 2]

$$T_{re} = \left( \frac{43}{11 g_*^{re}} \right)^{1/3} \left( \frac{a_0 H_{end}}{k} \right) e^{-(N_k + N_{re})} T_0, \quad (0.9)$$

Where, the use has been made of the relation  $a_k H_k = a_0 H_0$  for  $k$  being CMB pivot scale,  $k/a_0 = 0.05 \text{ Mpc}^{-1}$ .  $T_0 = 2.725^0 \text{ K}$  is the present CMB temperature.

**Model independent constraints:** The Eq.0.8 along with Eq.0.9 is one of our most important results, which indicates that the reheating temperature is determined completely by the inflationary parameters, ( $\omega_\phi, H_{end}, m_\phi^{end}$ ). Here, we first discuss the generic bounds on de-Sitter type inflation without specifying any particular model. Using the following approximate relation  $m_\phi^{end} \simeq \sqrt{(1+\omega_\phi)(4+12\omega_\phi)/(1-\omega_\phi)^2} H_{end}$  (under the assumption  $\phi_{end} \sim M_p$ ), one immediately gets  $\omega_\phi$  within (0.60, 0.99) and  $H_{end}$  within ( $1 \times 10^9, 5 \times 10^{13}$ ) GeV. This narrow and closed bound are derived from the minimum reheating temperature  $T_{re}^{min} = T_{BBN} = 10^{-2} \text{ GeV}$  and maximum possible value of the de-sitter Hubble scale at the end of inflation,  $H_{end}^{max} \simeq \pi M_p \sqrt{r A_s/2}$  calculated at upper limit on  $r = 0.036$  [15] (see Fig.1). Using these bounds GRe predicts reheating temperature to be  $T_{re} \lesssim 10^8 \text{ GeV}$ . Furthermore, using Eq.0.9 we found that inflationary e-folding number  $N_k$  has to be within a very narrow range (62, 63). *Therefore, to have successful GRe, viable de-Sitter inflation models will be those, which give  $N_k \sim (62, 63)$ , reheating EoS closer towards kination and predict reasonably low values of  $T_{re}$ .* This is indeed the case as we will discuss for  $\alpha$ -attractor.

**Model dependent constraints:** In order to see how GRe

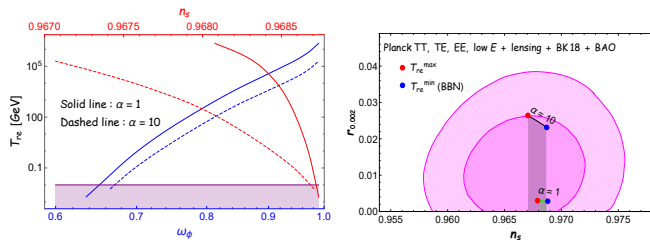


FIG. 1: **Left panel:** Variation of  $T_{re}$  as a function  $\omega_\phi$  (blue line) and  $n_s$  (red line). The purple region below  $10^{-2}$  GeV is forbidden from BBN bound. **Right panel:** Compare our result with the observational 68% and 95% CL constraints from BICEP/Keck, in the  $(n_s, r)$  plane.

can constrain the  $\alpha$ -attractor model, we numerically solve all the equations and the bounds on the model parameters are found to be,  $\{(200 \geq n \geq 4.75), (200 \geq n \geq 5.15)\}$  and  $\{(0.9681 \leq n_s \leq 0.9687), (0.9671 \leq n_s \leq 0.9687)\}$  for  $\alpha = (1, 10)$  and can be decoded from Fig.1. The bounds are well within the  $1\sigma$  range of  $n_s = 0.9649 \pm 0.0042$  (68 % CL, Planck TT,TE,EE+lowE+lensing) from Planck [14]. CMB normalization  $A_S \sim 10^{-9}$  is the only observed quantity that has been used in the above computation. The reheating temperature turned out to be bounded within  $10^{-2}\text{GeV} \leq T_{re} \leq 2 \times 10^6\text{GeV}$  for  $\alpha = 1$  and  $10^{-2}\text{GeV} \leq T_{re} \leq 2 \times 10^5\text{GeV}$  for  $\alpha = 10$ , where the lower limit is set by BBN (see Fig.1). Maximum  $T_{re}$  predicted by the inflation model turns out to be consistent with the model independent bound  $T_{re} < 10^8$  GeV. Finally, model predicts  $N_k$  within  $\{(62.5, 63.3), (64.6, 64.9)\}$  for  $\alpha = (1, 10)$  accordingly. In our following discussions, we will consider all the above bounds to derive the DM mass.

**DM phenomenology:** In particle physics, DM is still an ill-understood subject. Experimental direct detection proves to be challenging due to its unknown but tiny interaction with the nucleons. However, if the interaction is only gravitational, which is explicitly known, we may need to go beyond the conventional methods of detecting it. Planckian interacting dark matter has recently gained interest in the literature [10, 11]. In our GRe scenario, similar to radiation, dark matter is also coupled with inflaton suppressed by Planck mass. Therefore, DM mass  $m_Y$  is the only free parameter. Interestingly such scenarios naturally fix the DM mass through its abundance and inflaton model under consideration. Dynamics of DM is governed by [cf.Eq.(0.1)]

$$d(n_Y A^3) = \frac{\Gamma_{\phi\phi \rightarrow YY}}{m_\phi} \frac{\rho_\phi (1 + \omega_\phi)}{H} A^2 dA. \quad (0.10)$$

One should note that  $\Gamma_{\phi\phi \rightarrow ff}^{DM} \propto \rho_\phi/m_\phi$ , which makes fermion production slower compared to bosonic one during reheating. However, production of both DMs and radiation are expected to be completed well before the end of reheating. As a result the comoving  $(n_Y, \rho_R)$  become constant at reheating end. Therefore, present DM

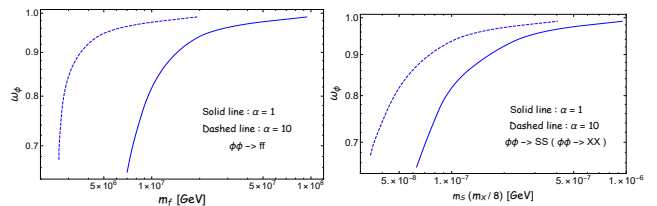


FIG. 2: Variation of  $\omega_\phi$  with respect to DM mass.

abundance can be safely calculated at the reheating end and is expressed as

$$\Omega_Y h^2 = \frac{m_Y n_Y (A_{re}) A_{re}^3}{\rho_R (A_{re}) A_{re}^4} \frac{A_{re} T_{re}}{T_0} \Omega_R h^2 = 0.12, \quad (0.11)$$

$\Omega_R h^2 = 4.16 \times 10^{-5}$  is the present radiation abundance. After straightforwardly integrating the Eq.0.1, one finds the comoving DM number density,  $n_Y^{com} = n_Y A_{re}^3$ , at the end of reheating for *fermion* and scalar/vector,

$$n_f^{com} \simeq \frac{3H_{end}^3}{2048\pi} \frac{1 + \omega_\phi}{1 - \omega_\phi} \left( \frac{m_f}{m_\phi^{end}} \right)^2 \left( 1 - e^{-\frac{3N_{re}}{2}(1 - \omega_\phi)} \right),$$

$$n_S^{com} = 8n_X^{com} = \frac{3H_{end}^3 (1 + \omega_\phi)}{512(\pi + 3\pi\omega_\phi)}, \quad (0.12)$$

respectively. Now, using this comoving number densities and the abundance Eq.0.11 we constrain the DM mass.

Model independent constraints on  $m_Y$ : We have already obtained the model independent constraint on  $(H_{end}, \omega_\phi)$  on which  $\Omega_Y h^2$  depends explicitly through Eqs.0.12. Therefore, successful GRe along with the correct DM relic abundance immediately put tight constraints on the allowed mass range for fermionic DM as,  $2 \times 10^5 \text{ GeV} \leq m_f \leq 3 \times 10^8 \text{ GeV}$ , and for scalar/vector DM as  $50 \text{ eV} \leq m_S, \gamma m_X \leq 1000 \text{ GeV}$ . Origin of higher  $m_f$  can be understood from the additional mass suppression  $(m_Y/m_\phi)^2$  in the  $\phi\phi \rightarrow ff$  decay width, which suppresses the fermionic DM number density. This requires enhanced value of  $m_f$  to satisfy the abundance.

Model dependent constraints on  $m_Y$ : Considering  $\alpha = (1, 10)$  in the Fig.2 we plotted  $(m_Y \text{ Vs } \omega_\phi)$  within the allowed range of  $\omega_\phi$  obtained previously. Important point to realize from the figure that for a specific value of  $\omega_\phi$  DM mass is unique. The allowed fermionic masses turned out to be within  $\{(7 \times 10^6, 9 \times 10^7), (3 \times 10^6, 2 \times 10^7)\}$  GeV for  $\alpha = (1, 10)$ . For bosonic DM, it is within  $\{(60, 1000), (30, 400)\}$  eV for  $\alpha = (1, 10)$ . Therefore, addition to selecting limited class of inflation models successful GRe predicts DM mass  $m_Y$  within a very narrow range of values.

**PGWs and constraints:** PGWs, (see Refs.[19–22]) is one of the profound predictions of inflation. It plays as a unique probe of the early universe. Particularly, the evolution of GWs and its amplitude are sensitive to the inflationary energy scale and the post inflationary EoS of the universe. Extremely weak coupling with matter fields helps PGWs to carry precise information about

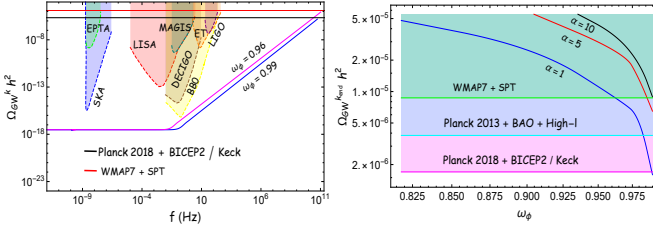


FIG. 3: **Left panel** : Behavior of  $\Omega_{GW}^k$  over a wide a range of frequency  $f = k/2\pi$  for  $\alpha = 1$ . **Right panel** :  $\Omega_{GW}^{k_{end}}$  Vs  $\omega_\phi$  for three different values of  $\alpha$  and the shaded regions are forbidden from three different BBN bounds.

its origin and subsequent evolution over a large cosmological time scale. Even though, we have not observed PGWs yet [23–28], simple cosmological upper bound on its strength during BBN will be shown to further tighten the bounds on the parameters discussed above. We focus on the behavior of PGWs spectrum for modes within  $k_{re} < k < k_{end}$  which re-enter the horizon during GRE after inflation.  $(k_{re}, k_{end})$  re-enter the horizon at the end of inflation and at the end of GRE respectively. Assuming GRE phase is dominated by  $\omega_\phi$ , the PGWs spectrum today is calculated as (see Ref.[29] for detailed derivation)

$$\Omega_{GW}^k h^2 \simeq \Omega_R h^2 P_T(k) \frac{4\mu^2}{\pi} \Gamma^2 \left( \frac{5 + 3\omega_\phi}{2 + 6\omega_\phi} \right) \left( \frac{k}{2\mu k_{re}} \right)^{n_{GW}} \quad (0.13)$$

Where,  $\mu = \frac{1}{2}(1 + 3\omega_\phi)$  and the index of the spectrum,  $n_{GW} = -(2 - 6\omega_\phi)/(1 + 3\omega_\phi)$ . The tensor power spectrum is,  $P_T(k) = H_{end}^2/12\pi^2 M_p^2$ . To this end we would like to state that for  $k < k_{re}$ , PGWs spectrum today is  $\Omega_{GW}^k h^2 \sim \Omega_R h^2 H_{end}^2/12\pi^2 M_p^2$ , which is scale-invariant for de-Sitter inflation. Eq.0.13 indicates that  $\Omega_{GW}^k$  increases with increasing  $k$  for  $\omega_\phi > 1/3$  (see Fig.3). Effective number of relativistic degrees of freedom during BBN place an upper limit on  $\Omega_{GW}^k$  (see Fig.3) [30]. We will analyze how this upper limit will give even tighter constraints on the parameters.

**Model independent constraints:** The maximum possible  $k = k_{end}$  and the relation  $k_{end}/k_{re} = \text{Exp}[N_{re}(-1 + 3\omega_\phi)/2]$  indicate  $\Omega_{GW}^{k_{end}} h^2$  being dependent only on  $(\omega_\phi, H_{end})$ , and hence provide further constraints in  $(\omega_\phi, H_{end})$ . Considering constraints on  $\Omega_{GW}^{k_{end}} h^2$  within  $(1.7 \times 10^{-6}, 8.4 \times 10^{-6})$  from different data set (see Fig.3), allowed range of EoS becomes  $0.97 < \omega_\phi \leq 0.99$ . This is much tighter compared to the constraints from GRE only and increasingly hinting towards the GRE phase being kination domination. This stringent constraint on  $\omega_\phi$  turned out to be consistent only with the inflationary e-folding number around  $N_k \simeq 62$ . Constraint on  $(H_{re}, T_{re}, m_f)$  remains nearly same as before, but scalar DM mass range further tightens into (400, 1000) eV.

**Model dependent constraints:** First panel of the Fig.3 suggests, if one considers most conservative bound on  $\Omega_{GW}^{k_{end}} h^2 \leq 1.7 \times 10^{-6}$  obtained from data set Planck-2018 + BICEP2/Keck array [31],  $\alpha = 1$  with  $\omega_\phi \simeq 0.99$

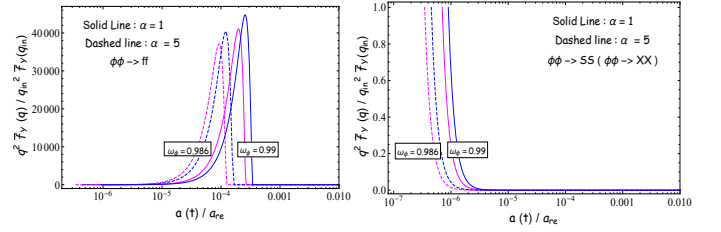


FIG. 4: Variation of rescaled PDFs of the dark matter as a function of  $a/a_{re}$  for different  $\omega_\phi$ .

appears to be the only allowed model which satisfies all the constraints. However, once relaxing the bound within  $(1.7 \times 10^{-6} \leq \Omega_{GW}^{k_{end}} \leq 8.4 \times 10^{-6})$  taking into account WMAP7[32] and SPT[33], allowed range of  $\omega_\phi$  get narrowed down within  $\{(0.96, 0.99), (0.986, 0.990)\}$  for  $\alpha = (1, 5)$  accordingly. Whereas, any  $\alpha > 10$  are completely excluded. Within the allowed value of  $\alpha = (1, 10)$ , maximum allowed range of scalar spectral index  $n_s$  becomes (0.9671, 0.9683), reheating temperature  $T_{re}$  becomes  $(2 \times 10^5, 2 \times 10^6)$  GeV, fermionic DM mass becomes  $(10^7, 10^8)$  GeV, and scalar/vector DM mass becomes (400, 1000) eV. However, all these ranges actually shrink towards their lower value as one goes from  $\alpha = 1 \rightarrow 10$ .

**Distinguishing the nature of DM:** So far, we have computed the background dynamics and associated constraints. In this section we will compute another important quantity called phase-space distribution functions (PDFs)  $f_Y(p_Y, t)$  which encodes the microscopic nature of DM and its production mechanism. We will see how,  $f_Y$  clearly distinguishes this which may leave imprints on DM halos mass function and matter power spectrum at present [34–36]. The PDFs for the gravitational dark matter satisfies,

$$\frac{\partial f_Y}{\partial t} - H p_Y \frac{\partial f_Y}{\partial p_Y} \simeq \frac{2\pi^2 \rho_\phi(t)}{m_\phi p_{Y0}^2} \Gamma_{\phi\phi \rightarrow Y Y} \delta(m_\phi - p_{Y0}) \quad (0.14)$$

where,  $(p_{Y0}, p_Y)$  are the energy and momentum associated with DM. Defining the rescaled distribution function  $\bar{f}_Y(q)$  as

$$f_Y(p_Y, t) = \frac{\pi^4 g_{re}}{15} \left( \frac{T_{re}}{m_\phi^{end}} \right)^4 \left( \frac{m_\phi^{re} a_{re}}{a} \right)^3 \bar{f}_Y(q). \quad (0.15)$$

Where, the rescaled comoving momentum  $q$  is expressed as  $q = p_Y a(t)/(m_\phi^{re} a_{re}) = (A(t)/A_{re})(m_\phi(t)/m_\phi^{re})$ , with  $m_\phi^{re}$  being inflaton mass at the end of reheating. Fig.4 reveals that scalar/vector dark matter PDFs attain its peak value at the beginning and then decay in terms of scale factor as  $q^2 f_s(q, t) \propto (a^2 \rho_\phi^2)/(m_\phi H) \propto A^{-\frac{1}{2}(5+3\omega_\phi)}$ . Because of slow production, Fermionic DM PDFs,  $q^2 f_f(q, t) \propto (a^2 \rho_\phi^2)/(m_\phi^3 H) \propto A^{\frac{1}{2}(5-9\omega_\phi)}$ , increases until the production is kinematically forbidden,  $m_f > m_\phi$ . Therefore, peak appears for fermionic PDFs



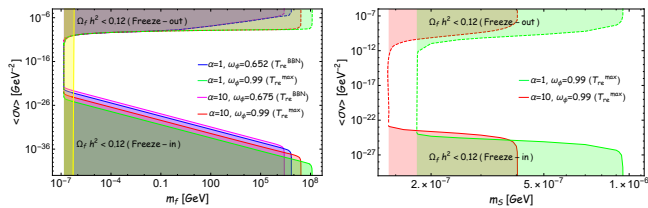


FIG. 5: Plot of  $\langle\sigma v\rangle$  Vs  $m_Y$  of fermionic (left panel) and scalar (right panel) DM. The Yellow band corresponds to minimum DM mass bound taken from [38].

at  $m_\phi(t) = m_Y$ . However, this distinguishing feature happens only for  $\omega_\phi > 5/9$  (see [3] for detailed discussions)

**Conclusions:** GRe mechanism appeared to be a unique physical scenario through which our present state of the universe is obtained after inflation. Being DM mass as the only free parameter, successful GRe put stringent constraint on the class of allowed models in the inflaton sector and predict very narrow window of DM mass. Considering available bounds on PGWs spectrum and DM abundance, GRe selects those inflation models which gives around unique  $N_k \sim 62$ , and inflaton EoS within  $0.97 < \omega_\phi \leq 0.99$  during reheating. Consequently reheating temperature must be  $T_{re} < 10^8$  GeV, fermionic DM mass should lie within  $2 \times 10^5$  GeV  $< m_f < 3 \times 10^8$  GeV, and scalar/vector DM mass within  $400$  eV  $< m_S, \gamma m_X < 1000$  eV. The results just mentioned above are obtained without specifying any model except the generic de-Sitter type inflation. However, if we consider a specific model such as  $\alpha$ -attractor, more narrower bounds are obtained due to its small prediction of  $r$ .  $\alpha$  turned out to be strictly bounded within (1, 10). Furthermore,  $n_s$  strictly lies within (0.9671, 0.9683),  $T_{re}$  lies within ( $2 \times 10^5, 2 \times 10^6$ ) GeV, fermionic DM mass lies within ( $10^7, 10^8$ ) GeV, and scalar/vector DM mass lies within (400, 1000) eV. To this end, let us point out that if we take into account the modified decay widths properly accounting for the oscillating inflaton zero-mode [5], all our predictions remain quantitatively the same except the fermionic DM mass range shifted towards the lower value by one order.

So far, all GRe predictions seem to be independent of any new physics in the radiation sector. However, if DM sector couples directly with the radiation bath with thermally averaged cross-section times velocity  $\langle\sigma v\rangle$ , then the DM masses obtained previously transformed into maximum one  $m_Y^{max}$  in  $(\langle\sigma v\rangle, m_Y)$  space [3] (see Fig.5). Upon decreasing DM mass, to our surprise, the existence of nearly model-independent minimum DM mass  $m_Y^{min}$  is observed where freeze-in and freeze-out mechanisms meet together. Such observation was also never reported before in the literature. This phenomenon is expected as decreasing  $m_Y$  requires increasing  $\langle\sigma v\rangle$  during freeze-in, and at its threshold value  $m_Y^{min}$  the DM thermalizes with radiation bath where freeze-out begins. The value of  $m_Y^{min}$  turned out as  $\sim 150$  eV for

fermion DM irrespective of model parameters. However, for fermionic DM, the most compact DM-dominated object called dwarf spheroidal galaxies are known to provide the lowest bound (Tremaine-Gunn (TG) bound) on its mass  $m_f \geq 590$  eV at 68% CL [38] shown in yellow shaded region. Finally, we want to point again that  $m_Y^{max}$  is set to be the maximum possible DM mass for both freeze-in ( $\langle\sigma v\rangle \rightarrow 0$ ) and freeze-out ( $\langle\sigma v\rangle \rightarrow \infty$ ) scenarios if one satisfies the present DM abundance. Therefore, if DM with  $m_Y > m_Y^{max}$  is detected, it will rule out the possibility of purely gravitational reheating after inflation.

- 
- [1] L. Dai, M. Kamionkowski and J. Wang, Phys. Rev. Lett. **113**, 041302 (2014)
  - [2] J. L. Cook, E. Dimastrogiovanni, D. A. Easson and L. M. Krauss, JCAP **04**, 047 (2015)
  - [3] M. R. Haque and D. Maity, [arXiv:2112.14668 [hep-ph]].
  - [4] M. Garny, M. Sandora and M. S. Sloth, Phys. Rev. Lett. **116**, no.10, 101302 (2016)
  - [5] S. Clery, Y. Mambrini, K. A. Olive and S. Verner, [arXiv:2112.15214 [hep-ph]].
  - [6] G. F. Giudice, E. W. Kolb and A. Riotto, Phys. Rev. D **64**, 023508 (2001)
  - [7] J. F. Donoghue, Phys. Rev. D **50**, 3874-3888 (1994)
  - [8] S. Y. Choi, J. S. Shim and H. S. Song, Phys. Rev. D **51**, 2751-2769 (1995)
  - [9] B. R. Holstein, Am. J. Phys. **74**, 1002-1011 (2006)
  - [10] Y. Mambrini and K. A. Olive, Phys. Rev. D **103**, no.11, 115009 (2021)
  - [11] B. Barman and N. Bernal, JCAP **06**, 011 (2021)
  - [12] R. Kallosh and A. Linde, JCAP **07**, 002 (2013)
  - [13] R. Kallosh, A. Linde and D. Roest, JHEP **11**, 198 (2013)
  - [14] Y. Akrami *et al.* [Planck], Astron. Astrophys. **641**, A10 (2020)
  - [15] P. A. R. Ade *et al.* [BICEP and Keck], Phys. Rev. Lett. **127**, no.15, 151301 (2021)
  - [16] J. Ellis, M. A. G. Garcia, D. V. Nanopoulos, K. A. Olive and S. Verner, [arXiv:2112.04466 [hep-ph]].
  - [17] J. Ellis, D. V. Nanopoulos and K. A. Olive, JCAP **10**, 009 (2013)
  - [18] M. Drewes, J. U. Kang and U. R. Mun, JHEP **11**, 072 (2017)
  - [19] L. P. Grishchuk, Zh. Eksp. Teor. Fiz. **67**, 825-838 (1974)
  - [20] A. A. Starobinsky, JETP Lett. **30**, 682-685 (1979)
  - [21] M. C. Guzzetti, N. Bartolo, M. Liguori and S. Matarrese, Riv. Nuovo Cim. **39**, no.9, 399-495 (2016)
  - [22] C. Caprini and D. G. Figueroa, Class. Quant. Grav. **35**, no.16, 163001 (2018)
  - [23] B. P. Abbott *et al.* [LIGO Scientific and Virgo], Phys. Rev. Lett. **118**, no.12, 121101 (2017) [erratum: Phys. Rev. Lett. **119**, no.2, 029901 (2017)]
  - [24] M. Punturo, M. Abernathy, F. Acernese, B. Allen, N. Andersson, K. Arun, F. Barone, B. Barr, M. Barsuglia and M. Beker, *et al.* Class. Quant. Grav. **27**, 194002 (2010)
  - [25] J. Crowder and N. J. Cornish, Phys. Rev. D **72**, 083005 (2005)
  - [26] N. Seto, S. Kawamura and T. Nakamura, Phys. Rev. Lett. **87**, 221103 (2001)
  - [27] P. Amaro-Seoane *et al.* [LISA], [arXiv:1702.00786 [astro-ph.IM]].

- [28] G. Janssen, G. Hobbs, M. McLaughlin, C. Bassa, A. T. Deller, M. Kramer, K. Lee, C. Mingarelli, P. Rosado and S. Sanidas, *et al.* PoS **AASKA14**, 037 (2015)
- [29] M. R. Haque, D. Maity, T. Paul and L. Sriramkumar, Phys. Rev. D **104**, no.6, 063513 (2021)
- [30] L. Pagano, L. Salvati and A. Melchiorri, Phys. Lett. B **760**, 823-825 (2016)
- [31] T. J. Clarke, E. J. Copeland and A. Moss, JCAP **10**, 002 (2020)
- [32] E. Komatsu *et al.* [WMAP], Astrophys. J. Suppl. **192**, 18 (2011)
- [33] R. Keisler, C. L. Reichardt, K. A. Aird, B. A. Benson, L. E. Bleem, J. E. Carlstrom, C. L. Chang, H. M. Cho, T. M. Crawford and A. T. Crites, *et al.* Astrophys. J. **743**, 28 (2011)
- [34] A. Boyarsky, J. Lesgourgues, O. Ruchayskiy and M. Viel, Phys. Rev. Lett. **102**, 201304 (2009)
- [35] M. R. Lovell, V. Eke, C. S. Frenk, L. Gao, A. Jenkins, T. Theuns, J. Wang, D. M. White, A. Boyarsky and O. Ruchayskiy, Mon. Not. Roy. Astron. Soc. **420**, 2318-2324 (2012)
- [36] R. Murgia, A. Merle, M. Viel, M. Totzauer and A. Schneider, JCAP **11**, 046 (2017)
- [37] S. Tremaine and J. E. Gunn, Phys. Rev. Lett. **42**, 407-410 (1979)
- [38] J. Alvey, N. Sabti, V. Tiki, D. Blas, K. Bondarenko, A. Boyarsky, M. Escudero, M. Fairbairn, M. Orkney and J. I. Read, Mon. Not. Roy. Astron. Soc. **501**, no.1, 1188-1201 (2021)